A closer look at using quasar near-zones as a probe of neutral hydrogen in the intergalactic medium

James S. Bolton[1]⋆ and Martin G. Haehnelt[2]

[1]*Max Planck Institut für Astrophysik, Karl-Schwarzschild Str. 1, 85748 Garching, Germany*
[2]*Institute of Astronomy, University of Cambridge, Madingley Road, Cambridge, CB3 0HA*

ABSTRACT

We examine a large set of synthetic quasar spectra to realistically assess the potential of using the relative sizes of highly ionized near-zones in the Lyα and Lyβ forest as a probe of the neutral hydrogen content of the intergalactic medium (IGM) at $z > 6$. The scatter in the relative near-zone size distribution, induced by underlying fluctuations in the baryonic density field and the filtering of ionizing radiation, is considerable even for fixed assumptions about the IGM neutral fraction. As a consequence, the current observational data cannot distinguish between an IGM which is significantly neutral or one which is highly ionized just above $z = 6$. Under standard assumptions for quasar ages and ionizing luminosities, a future sample of several tens of high-resolution Lyα and Lyβ near-zone spectra should be capable of distinguishing between a volume-weighted neutral hydrogen fraction in the IGM which is greater or less than 10 per cent.

Key words: radiative transfer – methods: numerical – H II regions – intergalactic medium – quasars: absorption lines – cosmology: theory.

1 INTRODUCTION

Quasar absorption spectra are currently the premier observational probe of the hydrogen reionization epoch. The average amount of Lyman series absorption observed in quasar spectra is consistent with an intergalactic medium (IGM) with a volume-weighted neutral hydrogen fraction in excess of $\langle f_{\rm H\,I} \rangle_{\rm V} \sim 10^{-3.5}$ at $z \simeq 6$ (Fan et al. 2006b; Becker, Rauch & Sargent 2006). However, obtaining more stringent constraints on the IGM neutral hydrogen fraction using this technique at $z > 6$ is extremely difficult; larger neutral fractions produce saturated Lyman series absorption over substantial regions in the spectra of these quasars, the observational manifestation of which is the Gunn & Peterson (1965) trough.

Consequently, several techniques which may be sensitive to larger values of $\langle f_{\rm H\,I} \rangle_{\rm V}$ have been proposed (see Fan, Carilli & Keating 2006a, and references therein). The sizes of transparent regions observed immediately blueward of the Lyα emission line of $z > 6$ quasars, if equivalent to the size of the H II regions surrounding the quasars, should be proportional to the ambient IGM neutral hydrogen fraction when adopting assumptions for the quasar age and ionizing luminosity (Cen & Haiman 2000; Madau & Rees 2000; Yu & Lu 2005). Under these assumptions, these regions are consistent with $\langle f_{\rm H\,I} \rangle_{\rm V} > 0.1$, just above $z = 6$ (Wyithe & Loeb 2004; Wyithe, Loeb & Carilli 2005), although a recent independent analysis including modelling of the Gunn–Peterson trough damping wing by

Mesinger & Haiman (2007) using many simulated quasar sight-lines favours a slightly lower limit of $\langle f_{\rm H\,I} \rangle_{\rm V} > 0.033$.

However, recent numerical studies which correctly model the radiative transfer of ionizing photons around these quasars indicate that interpreting the sizes of these highly ionized Lyα near-zones with respect to the neutral hydrogen content of the IGM is complicated (Bolton & Haehnelt 2007a; Maselli et al. 2007; Lidz et al. 2007). There are two main reasons for this, in addition to the uncertain quasar age and ionizing luminosity. First, for small neutral fractions the Lyα near-zone resembles the classical proximity zone of a luminous quasar embedded in a highly ionized IGM (Bajtlik, Duncan & Ostriker 1988) and does not correspond to the extent of an H II region expanding into a substantially neutral IGM. The observationally identified Lyα near-zone sizes can then substantially underestimate the size of the region of enhanced ionization surrounding the quasar, leading to an overestimation of the IGM neutral hydrogen fraction. Secondly, even for fixed assumptions about the ionization state of the IGM, variations in the IGM density and the ionizing background along different quasar sight-lines combined with radiative transfer effects lead to a considerable scatter in the near-zone sizes. Drawing robust constraints on $\langle f_{\rm H\,I} \rangle_{\rm V}$ from only a small sample of spectra is therefore difficult. Bolton & Haehnelt (2007a) found the observed near-zone sizes at $z > 6$ are consistent with neutral hydrogen fractions as small as $\langle f_{\rm H\,I} \rangle_{\rm V} = 10^{-3.5}$.

Nevertheless, further progress may be possible by also considering the size of the corresponding Lyβ near-zone. The edge of the Lyβ near-zone should trace the position of the quasar H II ionization front (IF) to smaller volume-averaged neutral hydrogen fractions in

⋆E-mail: jsb@mpa-garching.mpg.de

the ambient IGM relative to the Lyα near-zone. The difference in the sizes of these regions thus holds additional information on the IGM neutral hydrogen fraction (Mesinger & Haiman 2004; Bolton & Haehnelt 2007a, hereafter BH07a). In principle, the ratio of Lyβ to Lyα near-zone sizes should increase from unity to a maximum value of ~2.5 as the IGM neutral hydrogen fraction decreases (BH07a). In practice, however, the ratio can be much smaller than 2.5 even for very small neutral fractions and it will exhibit a large scatter due to fluctuations in the IGM density along the line of sight.

In this Letter we extend the work of BH07a to examine the use of Lyα and Lyβ near-zones as a probe of $\langle f_{\rm H\,I}\rangle_{\rm V}$. Our work closely follows on from the concepts discussed in BH07a, although the analysis presented here differs in three important ways. We analyse several hundred different simulations of the radiative transfer of ionizing photons around $z > 6$ quasars, greatly improving the synthetic spectra statistics. An approximate treatment of an inhomogeneous ionizing background, expected towards the tail end of hydrogen reionization (Fan et al. 2006b; Wyithe & Loeb 2006), is now also included within the radiative transfer simulations. Lastly we adopt a more robust method for defining the sizes of both Lyα and Lyβ near-zones. As a consequence, we are able to more realistically assess the potential of using quasar near-zones as a probe of the IGM neutral hydrogen fraction beyond $z = 6$.

2 SIMULATIONS

2.1 Radiative transfer implementation and the IGM density distribution

We use the one-dimensional, multifrequency photon-conserving algorithm described and tested in BH07a to compute the radiative transfer of ionizing photons around quasars. This is combined with density distributions drawn from the 400^3 hydrodynamical simulation of BH07a, run using the parallel TREE-SPH code GADGET-2 (Springel 2005). The 10 most massive haloes in the simulation at $z = 6.25$ were identified and baryon density distributions were extracted in different orientations around them. Continuous density distributions $150\,h^{-1}$ comoving Mpc in length were then constructed using the halo density distributions combined with other sight-lines drawn randomly from the simulation volume. One end of the density distributions always lies at the centre of one of the identified haloes, where the quasar is assumed to reside during the radiative transfer calculation. This process was repeated to produce 240 unique sight-lines.

Synthetic Lyα and Lyβ spectra are constructed from the output of the radiative transfer simulations following standard procedure (e.g. BH07a). The raw synthetic spectra are processed to resemble data obtained with the Keck telescope Echelle Spectrograph and Imager (ESI). The spectra are convolved with a Gaussian with a full width half maximum (FWHM) of $66\,{\rm km\,s^{-1}}$ and rebinned on to pixels of width 3.5 Å ($R \sim 2500$). Gaussian distributed noise is then added with a total signal-to-noise ratio of 20 per pixel at the continuum level and a constant read-out signal-to-noise ratio of 80 per pixel. We also process some of the spectra to resemble data taken with the Keck telescope High Resolution Echelle Spectrometer (HIRES). These are convolved with a Gaussian with a FWHM of $7\,{\rm km\,s^{-1}}$ and rebinned on to pixels of width 0.25 Å ($R \sim 35\,000$). Noise is then added with a total signal-to-noise ratio of 20 per pixel at the continuum level and a constant read-out signal-to-noise of 100 per pixel.

Random sight-lines were also drawn from the simulation at $z = 5.12$ to model the foreground Lyα forest superimposed on the Lyβ

absorption at $z = 6.25$. These were spliced together to produce a $z = 5.12$ Lyα spectrum with the same wavelength coverage as the Lyβ spectrum at $z = 6.25$. Lastly, the foreground Lyα optical depths are rescaled (e.g. Bolton & Haehnelt 2007b) to reproduce the observed mean flux of the Lyα forest at $z = 5.12$, $\langle F\rangle = 0.149$ (Songaila 2004).

2.2 Initial conditions and the fluctuating ionizing background model

We run a total of 480 radiative transfer simulations arranged into two groups of 240 simulations. The density distributions for both groups have initial neutral hydrogen fractions distributed uniformly in the range $-4 \lesssim \log\langle f_{\rm H\,I}\rangle_{\rm V} \lesssim 0$, set by assuming that the IGM is in ionization equilibrium with an ionizing background with a power-law spectral index, $\alpha_{\rm b} = 3$, below the Lyman limit. For the first group of 240 simulations the ionizing background is assumed to be spatially uniform, as in BH07a.

However, a spatially uniform ionizing background is likely to be a poor approximation at the tail end of reionization and this assumption may have an impact on the near-zone sizes derived from simulations (Lidz et al. 2007; Alvarez & Abel 2007). Therefore, for the second group of simulations we construct spatially fluctuating ionizing backgrounds using observationally determined Lyman break galaxy (LBG) luminosity functions at high redshift. We do this using the model of Bolton & Haehnelt (2007b), to which we refer the reader for further details. An example of the fluctuating photoionization rate per hydrogen atom, $\Gamma_{\rm H\,I}$, along a single sight-line at $z = 6.25$ is shown in Fig. 1. The background value of $\Gamma_{\rm H\,I}$ due to galaxies is several orders of magnitude larger in overdense regions due to the clustering of ionizing sources, although it is still dominated by the quasar radiation field within 10 proper Mpc of the host halo. In order to reproduce different initial values of $\langle f_{\rm H\,I}\rangle_{\rm V}$ in our simulations we rescale the mean of the fluctuating ionization rate along each sight-line by the appropriate amount. Note, however, that this simple model only applies during the post-overlap phase of
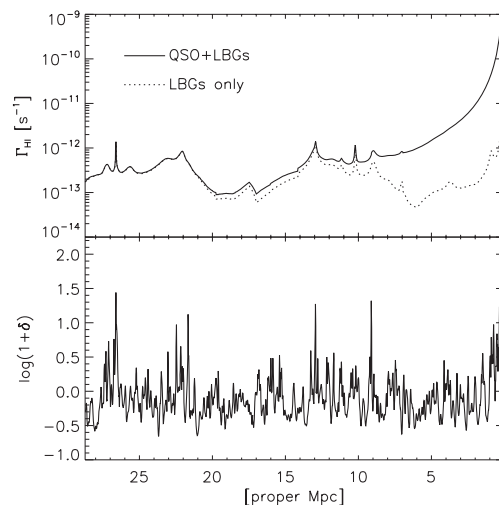

Figure 1. Top: example of the spatially fluctuating hydrogen ionization rate along a simulated quasar sight-line. The quasar is situated at the right-hand side of the diagram. The dotted line shows the ionizing background due to galaxies only and the solid line also includes the contribution from the quasar computed using the radiative transfer implementation. Bottom: the corresponding baryonic overdensity along the sight-line. The ionizing background is enhanced in overdense regions due to the clustering of ionizing sources.

reionization (cf. Gnedin 2000) when the ionizing photon mean free path is larger than the typical separation between ionizing sources. For a mean free path which is shorter than the typical ionizing source separation, large values of $\langle f_{\rm HI}\rangle_{\rm V}$ can also be produced by the presence of small, highly ionized regions surrounded by an entirely neutral IGM (Lidz et al. 2007; Alvarez & Abel 2007). We discuss the possible impact of these pre-ionized regions on near-zone sizes later in this Letter.

The fiducial quasar parameters adopted in the radiative transfer simulations are an ionizing photon production rate of $\dot{N} = 2 \times 10^{57}$ s^{-1}, an age of $t_{\rm Q} = 10^7$ yr and a power-law spectral index of $\alpha_{\rm s} = 1.5$ below the Lyman limit. The value of $\dot{N}$ is consistent with the $z > 6$ quasar luminosities inferred by Fan et al. (2006b) and independently constrained by Mesinger & Haiman (2007). Quasar ages are rather more uncertain, although 10^7 yr is in agreement within current observational constraints (Martini 2004) and theoretical models (Hopkins et al. 2006). The impact of differing values of $\dot{N}$ and $t_{\rm Q}$ on the sizes of quasar near-zones is discussed in detail in BH07a.

3 RESULTS

3.1 A consistent definition for Lyα and Lyβ near-zone sizes

There are considerable variations in Lyα and Lyβ near-zone sizes even for fixed values of $\langle f_{\rm HI}\rangle_{\rm V}$ due to underlying fluctuations in the IGM density field. Therefore, a consistent definition for the sizes of the Lyα and Lyβ near-zones is very important when comparing individual spectra. Fan et al. (2006b) smoothed the observed Lyα near-zone spectra to a resolution of 20 Å and identified the near-zone sizes at the first pixel which dropped below a normalized flux threshold of $F = 0.1$. However, this definition is not suitable for the Lyβ near-zone, where the transmission is much weaker and more patchy due to the foreground Lyα forest. Alternatively, BH07a measured Lyα and Lyβ near-zone sizes at the position where the last pixel in an unsmoothed spectrum drops below a normalized flux threshold of $F = 0.1$. Although providing a better measure of the Lyβ near-zone size, this definition still breaks down once the IGM as a whole becomes highly ionized and the edge of the near-zones become ambiguous. To overcome these difficulties, we add the extra condition that the last pixel at which the flux drops below $F = 0.1$ must be followed by a gap of $\Delta z > 0.1$ where the normalized flux remains *below* the $F = 0.1$ threshold. Any spectra which do not meet this criterion are considered to have unidentifiable Lyα and Lyβ near-zones and are rejected from our analysis. This occurs for only one and three sight-lines in the synthetic ESI and HIRES samples, respectively.

3.2 The impact of ionizing background fluctuations on the sizes of near-zones

The sizes of the Lyα and Lyβ near-zones measured from our 480 synthetic ESI spectra are shown as the red diamonds in Fig. 2. The top panels show the sizes measured assuming a uniform ionizing background, while the bottom panels correspond to the sizes measured with the assumption of a spatially fluctuating ionizing background. We find a substantial scatter in the near-zone sizes even for fixed assumptions for $\langle f_{\rm HI}\rangle_{\rm V}$. The scatter is rather similar for the spectra computed with either a uniform or spatially fluctuating ionizing background, suggesting that differences in the density distribution and radiative transfer effects play a more important role in generating this variation. There is also little evidence that enhanced ionization in the overdense regions increases the average near-zone
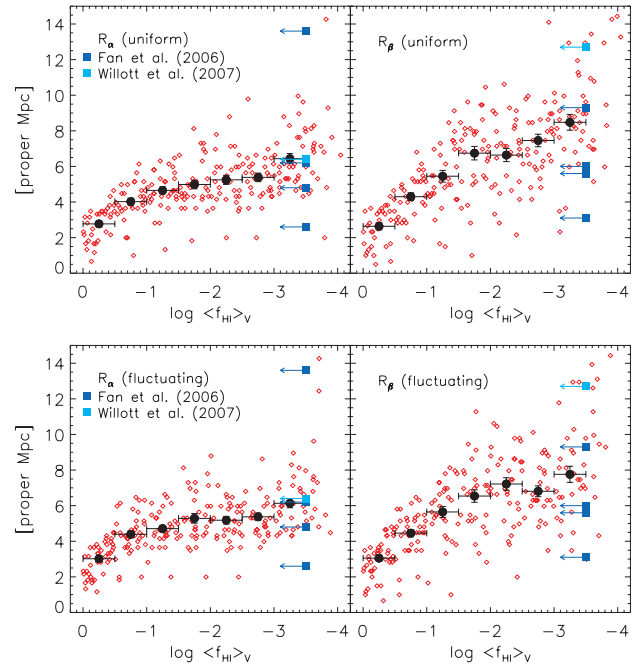

Figure 2. Top: the red diamonds correspond to Lyα (left-hand panel) and Lyβ (right-hand panel) near-zone sizes measured from 240 synthetic ESI spectra using the method described in Section 3.1. The data are plotted as a function of the volume-weighed neutral hydrogen fraction in the IGM. A spatially uniform ionizing background has been assumed. The filled black circles with 1σ error bars correspond to the average near-zone sizes in bins of width $\Delta[\log \langle f_{\rm HI}\rangle_{\rm V}] = 0.5$. Bottom: as for the top panel, except assuming a spatially fluctuating ionizing background. The filled blue and cyan squares in all panels correspond to near-zone sizes we derive from the published observational data, given in Table 1.

size. Note, however, that during the overlap-phase spatial fluctuations in the ionizing background are expected to be larger than we have assumed here and can extend over wider scales. This is due to the rapid increase of the mean free path for ionizing photons in the short phase when the ionized regions percolate.

The filled black circles with error bars in Fig. 2 correspond to the average near-zone sizes in bins of width $\Delta[\log \langle f_{\rm HI}\rangle_{\rm V}] = 0.5$. The error bars correspond to the 1σ standard error of the mean. There are three main regimes in the Lyα near-zone size as a function of $\log \langle f_{\rm HI}\rangle_{\rm V}$ for the quasar age and luminosity adopted here. The first is when $R_\alpha \propto \langle f_{\rm HI}\rangle_{\rm V}^{-1/3}$ for $\langle f_{\rm HI}\rangle_{\rm V} > 0.1$. In this regime the Ly$\alpha$ near-zone edge closely corresponds to the H II IF. The second regime is when the near-zone corresponds to a classical proximity zone and the size is independent of the neutral fraction; in this case the H II IF actually lies ahead of the Lyα near-zone edge but the residual neutral hydrogen behind it is large enough to produce saturated Lyα absorption. Lastly, for $\langle f_{\rm HI}\rangle_{\rm V} < 10^{-3.5}$ the measured Lyα near-zone sizes increase again due to additional transmission originating from regions now highly ionized by the ionizing background. The Lyβ near-zones exhibit a similar trend to the Lyα data, except due to the smaller Lyβ absorption cross-section they are able to trace the position of the H II IF to lower IGM neutral hydrogen fractions, reaching $R_\beta \propto \langle f_{\rm HI}\rangle_{\rm V}^0$ at $\langle f_{\rm HI}\rangle_{\rm V} \simeq 10^{-2}$. Therefore, as noted by BH07a (but see also Mesinger & Haiman 2004, for a different interpretation), evidence for $R_\beta/R_\alpha > 1$ may provide an interesting constraint on $\langle f_{\rm HI}\rangle_{\rm V}$.

Finally, we plot the Lyα and Lyβ near-zone sizes we measured from the five quasars at $z > 6.1$ with published spectra as filled blue

Table 1. The Lyα and Lyβ near-zone sizes around the five quasars with published spectra at $z > 6.1$. The sizes have been measured from the spectra using the definition given in Section 3.1.

Quasar	R_α [proper Mpc]	R_β [proper Mpc]	R_β/R_α
J1509−1749	6.4 ± 1.2	12.7 ± 1.2	2.0
J1250+3130	13.6 ± 1.2	9.3 ± 1.2	0.7
J1623+3192	2.6 ± 1.0	3.1 ± 1.0	1.2
J1030+0524	4.8 ± 1.2	6.0 ± 1.2	1.2
J1148+5251	6.2 ± 1.4	5.6 ± 1.4	0.9

and cyan squares in Fig. 2 (Fan et al. 2006b; Willott et al. 2007). We have omitted J1030 + 0524 at $z = 6.2$ from this sample as this is a broad absorption line quasar which complicates the measurement of the near-zone size. Following Fan et al. (2006b), the sizes are rescaled to a common absolute magnitude of $M_{1450} = -27$ by assuming the near-zone size is proportional to $\dot{N}^{1/3}$, although $\dot{N}^{1/2}$ may be more appropriate (BH07a). This magnitude corresponds to $\dot{N} \simeq 1.9 \times 10^{57}$ s^{-1} for the quasar spectrum adopted in this work. The lower limit of $\langle f_{HI} \rangle_V \gtrsim 10^{-3.5}$ measured from the Gunn–Peterson trough limits is assumed. An uncertainty of $\Delta z = 0.02$ in the systemic redshift of the quasar is adopted when determining the systematic error on the near-zone sizes. We do not show the systematic uncertainties on the measured near-zone sizes in Fig. 2 for clarity, but the data are given in Table 1. The observational data exhibit a large scatter similar to that seen in the synthetic data, and are consistent with a wide range of neutral fractions.

3.3 Probing the neutral fraction with the ratio of Lyβ and Lyα near-zone sizes

A potentially interesting constraint on $\langle f_{HI} \rangle_V$ may be obtained by considering the ratio of the Lyβ to Lyα near-zone sizes. The red diamonds in the left-hand panel of Fig. 3 correspond to R_β/R_α as a function of $\log \langle f_{HI} \rangle_V$ for the synthetic ESI spectra constructed using the fluctuating ionizing background model. The filled black circles show the average values of R_β/R_α in bins of width $\Delta[\log \langle f_{HI} \rangle_V] = 0.5$. The error bars correspond to the 1σ standard error of the mean. The earlier analysis by BH07a found $R_\beta/R_\alpha > 1$ was consistent
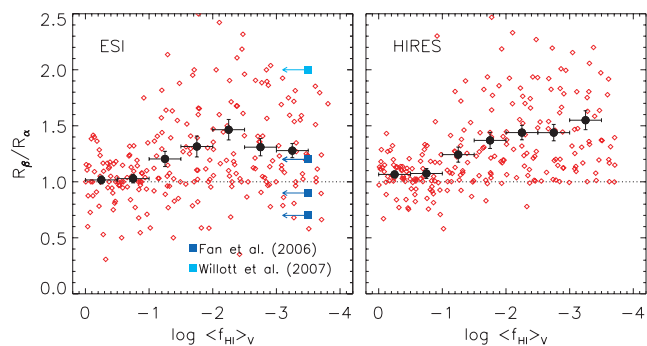

Figure 3. Left: the ratio of Lyβ to Lyα near-zone sizes as a function of the volume-weighted neutral hydrogen fraction, measured from synthetic ESI spectra constructed assuming a spatially fluctuating ionizing background. The red diamonds show the individual measurements and the filled black circles with 1σ error bars correspond to the averages in bins of width $\Delta[\log \langle f_{HI} \rangle_V] = 0.5$. The filled blue and cyan squares correspond to the near-zone sizes measured from the published data, given in Table 1. Right: as for the left-hand panel, except the data are now measured from synthetic HIRES spectra.

with $\langle f_{HI} \rangle_V \lesssim 10^{-2}$. However, this was based on a small sample of 20 synthetic spectra which used only four different initial values of $\langle f_{HI} \rangle_V$. The improved statistics and wider sampling of $\langle f_{HI} \rangle_V$ in this work indicate $R_\beta/R_\alpha > 1$ when $\langle f_{HI} \rangle_V \lesssim 0.1$ at the 3σ level for a sample of around 30 ESI spectra.

Assuming that $R_\beta/R_\alpha > 1$ is indeed consistent with $\langle f_{HI} \rangle_V \lesssim 0.1$, how reliable a constraint on $\langle f_{HI} \rangle_V$ can the current observational data provide? The observed near-zone sizes we measure from the published data (Fan et al. 2006b; Willott et al. 2007) at $z > 6.1$ are plotted as the filled blue and cyan squares in Fig. 3. Once again, the observational data are consistent with a wide range of $\langle f_{HI} \rangle_V$. The mean of the observational data favours a value of $R_\beta/R_\alpha = 1.2$, although with only five data points this result is certainly not a significant one. The simulated data indicates that about 20 ESI spectra would be required for a 2σ result. Obtaining reliable constraints on $\langle f_{HI} \rangle_V$ using this technique with the current data is probably not yet possible.

Higher resolution quasar spectra would enable a more accurate determination of the sizes of the Lyα and Lyβ near-zones. This is demonstrated in the right-hand panel of Fig. 3 in which our simulated spectra have been processed to resemble data taken with HIRES. The scatter in the data is significantly reduced with the higher resolution spectra. Strong evidence for a neutral fraction $\langle f_{HI} \rangle_V < 10^{-1}$ should be obtainable with a sample of 30 high-resolution spectra at the 3–5σ level.

3.4 The effect of quasar age, ionizing luminosity and surrounding galaxies

An important caveat to the argument presented in this work is that the $\langle f_{HI} \rangle_V$ threshold where $R_\beta/R_\alpha > 1$ becomes statistically significant is also degenerate with the age of a quasar, its ionizing luminosity and the size of any pre-existing ionized region around the quasar host halo. The observable $R_\beta/R_\alpha > 1$ corresponds to the $\langle f_{HI} \rangle_V$ threshold at which $R_{HII} > R_\alpha$, where R_{HII} is the extent of the H II IF. The position of the H II IF will scale approximately as $R_{HII} \propto \langle f_{HI} \rangle_V^{-1/3} \dot{N}^{1/3} t_Q^{1/3}$ but the saturated Lyα near-zone size will scale as $R_\alpha \propto \dot{N}^{1/2}$ only (BH07a). Therefore, if the mean quasar age is 10 times larger than the fiducial 10^7 yrs, the H II IF will be around twice as far from the quasar but the Lyα near-zone size will remain unchanged. The $\langle f_{HI} \rangle_V$ threshold corresponding to $R_\beta/R_\alpha > 1$ will thus be 10 times larger. Alternatively, a smaller quasar age will lower the $\langle f_{HI} \rangle_V$ threshold corresponding to $R_\beta/R_\alpha > 1$. Disentangling this quasar age and neutral fraction degeneracy from the data is potentially very difficult without a good independent estimate of the typical quasar age. Note, however, the degeneracy with $\dot{N}$ is less dramatic, as both the near-zone size and the H II IF position scale similarly with $\dot{N}$. Finally, luminous quasars are expected to be hosted by rather massive dark matter haloes and the reionization process may be further advanced in their immediate environment compared to a typical region of the Universe. If pre-existing ionized regions produced by clustered galaxies lower the local value of $\langle f_{HI} \rangle_V$ around these quasars, the IFs will travel further than one expects for a uniformly ionized IGM (Lidz et al. 2007; Alvarez & Abel 2007). The observed near-zone sizes may then exhibit $R_\beta/R_\alpha > 1$ even if $\langle f_{HI} \rangle_V > 0.1$.

4 CONCLUSIONS

We have carefully examined the potential of the ratio of Lyβ to Lyα near-zone sizes as a probe of the IGM H I fraction at $z > 6$

with a large set of detailed radiative transfer simulations. Adopting a robust, simultaneous definition for Lyα and Lyβ near-zone sizes, we find that a sample of around 30 ESI quasar spectra would be required to distinguish between an IGM which has an H I fraction greater or less than 10 per cent at the 3σ level. Unfortunately, the current observational data, consisting of five quasar spectra at $z >$ 6.1, are too few to place significant constraints on $\langle f_{\mathrm{H\,I}} \rangle_V$. Our results also suggest that, at least in the post-overlap phase of reionization, fluctuations in the ionizing background will have a negligible effect on near-zone sizes. However, if the typical quasar age is substantially longer than the canonical 10^7 yrs, or if pre-existing ionized regions surround quasar host haloes during the pre-overlap stage of reionization, it may still be very difficult to distinguish between a highly ionized or substantially neutral IGM. Attempts to disentangle the former effect from the data may benefit from alternative statistics, such as the detection of a Gunn–Peterson trough damping wing (Mesinger & Haiman 2004, 2007), while distinguishing the latter effect may be possible with a sample of $z > 6$ gamma ray burst (GRB) spectra, which should probe less biased regions compared to luminous quasars. However, only one such spectrum has been obtained so far (Totani et al. 2006) and its interpretation is hampered by damped Lyα absorption from neutral hydrogen in the GRB host galaxy.

High-resolution data significantly improves the ability to constrain the neutral fraction, and HIRES spectra of $z > 6$ quasars are already in existence (Becker, Sargent & Rauch 2005). Next-generation infrared surveys (see Lawrence 2007, for a recent review) such as the UKIRT Infrared Deep Sky Survey (UKIDSS) are expected to find several tens of new quasars at $z \simeq 6$ (Venemans et al. 2007). Future data sets should thus be able to provide an interesting limit on the IGM neutral hydrogen fraction from the relative sizes of Lyα and Lyβ near-zones.

REFERENCES

Alvarez M. A., Abel T., 2007, MNRAS, in press, (doi: 10.1111/j.1745-3933.2007.00342.x) (astro-ph/0703740)
Bajtlik S., Duncan R. C., Ostriker J. P., 1988, ApJ, 327, 570
Becker G. D., Rauch M., Sargent W. L. W., 2006, ApJ, 662, 72
Becker G. D., Sargent W. L. W., Rauch M., 2005, in Williams P., Shu C.-G., Menard B., eds, Proc. IAU Coll. 199, Probing Galaxies through Quasar Absorption Lines. Cambridge Univ. Press, Cambridge, p. 357
Bolton J. S., Haehnelt M. G., 2007a, MNRAS, 374, 493 (BH07a)
Bolton J. S., Haehnelt M. G., 2007b, MNRAS, submitted (astro-ph/0703306)
Cen R., Haiman Z., 2000, ApJ, 542, L75
Fan X., Carilli C. L., Keating B., 2006a, ARA&A, 44, 415
Fan X. et al., 2006b, AJ, 132, 117
Gnedin N. Y., 2000, ApJ, 535, 530
Gunn J. E., Peterson B. A., 1965, ApJ, 142, 1633
Hopkins P. F., Hernquist L., Cox T. J., Di Matteo T., Robertson B., Springel V., 2006, ApJS, 163, 1
Lawrence A., 2007, A&G, 48, 3.27
Lidz A., McQuinn M., Zaldarriaga M., Hernquist L., Dutta S., 2007, ApJ submitted (astro-ph/0703667)
Madau P., Rees M. J., 2000, ApJ, 542, L69
Martini P., 2004, in Ho L. C., ed., Carnegie Observatories Astrophysics Series Vol. 1, Coevolution of Black Holes and Galaxies. Cambridge Univ. Press, Cambridge, p. 169
Maselli A., Gallerani S., Ferrara A., Choudhury T. R., 2007, MNRAS, 376, L34
Mesinger A., Haiman Z., 2004, ApJ, 611, L69
Mesinger A., Haiman Z., 2007, ApJ, 660, 923
Songaila A., 2004, AJ, 127, 2598
Springel V., 2005, MNRAS, 364, 1105
Totani T., Kawai N., Kosugi G., Aoki K., Yamada T., Iye M., Ohta K., Hattori T., 2006, PASJ, 58, 485
Venemans B. P., McMahon R. G., Warren S. J., Gonzalez-Solares E. A., Hewett P. C., Mortlock D. J., Dye S., Sharp R. G., 2007, MNRAS, 376, L76
Willott C. et al. 2007, AJ, submitted (astro-ph/0706.0914)
Wyithe J. S. B., Loeb A., 2004, Nat, 432, 194
Wyithe J. S. B., Loeb A., 2006, ApJ, 646, 696
Wyithe J. S. B., Loeb A., Carilli C., 2005, ApJ, 628, 575
Yu Q., Lu Y., 2005, ApJ, 620, 31

This paper has been typeset from a TEX/LATEX file prepared by the author.